Active Fault-Tolerant Control for Discrete Vehicle Active Suspension via Reduced-Order Observer

Shi-Yuan Han, Jin Zhou, *Member, IEEE*, Yue-Hui Chen, Yi-Fan Zhang, *Member, IEEE*, Gong-You Tang, and Lin Wang, *Member, IEEE*

***Abstract*—In this article, the fault-tolerant control (FTC) problem of vehicle active suspension is concerned in the discrete-time domain, in which the road disturbances and faults in actuator and measurement are considered. The main contribution consists of proposing an active physically realizable fault-tolerant controller based on a reduced-order observer, which makes up an optimal vibration control component and an event-triggered FTC component. More specifically, by discussing a discrete vehicle active suspension subject to road disturbances generated from the output of a designed exosystem, the optimal vibration control component is derived from maximum principle to offset the inevitable vibrations. Meanwhile, based on the real-time system output of vehicle suspension rather than residual error, a reduced-order observer is proposed to cover the physically unrealizable problem for the designed optimal vibration control component. After that, an event-triggered FTC component and an event-triggered restructured system output are designed to compensate the faults in actuator and measurement, respectively. Finally, extensive experiments are conduced to the control performance of vehicle active suspension under the proposed controller, and confirm its effectiveness and superiority over other control schemes.**

***Index Terms*—Event-triggered control, fault-tolerant control (FTC), optimal vibration control, reduced-order observer, vehicle active suspension.**

I. Introduction

VEHICLE active suspension is of great significance for vehicle engineering to the overall vehicle performance. With the benefit of advanced actuator technologies combined with advanced control algorithms, it has huge advantages for satisfying the performance requirements in the wide frequency range, including the road holding ability, ride comfort, and suspension deflection [1]–[3]. In order to achieve the tradeoff among the conflicting performance requirements, combining active vibration control mechanism with advanced optimal control algorithms to attenuate the vibration has attracted continuing attention in the past decade. These studies include linear-quadratic optimal control [4], approximation optimal vibration control [5], stochastic optimal active control [6], and optimal preview active control [7]. It is worth noting that, the aforementioned suspension control schemes hold on the assumption that all suspension system status are with known quantities of values. However, due to the physical limitations and high implement cost of measurement technologies, it is impossible to monitor all necessary driving status directly [8], such as tire deflection and unsprung mass acceleration. Therefore, based on the incomplete status information of vehicle suspension, it is imperative to design an effective observer to estimate the precise values of all necessary suspension status for designing the reasonable optimal vibration controller.

From the viewpoint of application, vehicle active suspension is in imperfect working surroundings [9], [10]. Correspondingly, advanced suspension actuator can add or dissipate system energy thereby eliminating the harmful effects of the undesirable vibrations and improving the ride comfort and road holding ability [11]. However, due to the growing complexity of vehicle active suspension, the extended benefits are paralleled with the increasing possibility of component failures in actuator and measurement [12], [13]. What is worse, undesired vibrations and faults, if not properly controlled, may cause deterioration of suspension performance, and even cause damage and loss of life and property [14], [15]. Fortunately, for satisfying the requirements of the safety, reliability, and fault tolerance, the technologies of fault diagnosis (FD) and fault-tolerant control (FTC) are essential procedure during system design and automatic control [16]–[18]. Meanwhile, a great number of theoretic studies have been presented to address FTC problem for traditional control systems, including fuzzy adaptive control [19], H_∞ control [20], observer-based control [21]–[23], fuzzy neural network [24], model-based method [25], [26], and sliding mode control [27]. Admittedly, due to the negative effects from irregular road disturbances, it is a significant challenge to diagnose the fault signals in actuator and measurements for vehicle active suspension.

Manuscript received November 13, 2019; accepted December 26, 2019. This work was supported in part by the National Natural Science Foundation of China under Grant 61903156, Grant 61873324, and Grant 61872419, in part by the Natural Science Foundation of Shandong Province under Grant ZR2017MF044 and Grant ZR2019MF040, and in part by the Taishan Scholar Project of Shandong Province under Grant tsqn201812077. This article was recommended by Associate Editor M. P. Fanti. *(Corresponding author: Jin Zhou.)*

Shi-Yuan Han, Jin Zhou, Yue-Hui Chen, and Lin Wang are with the Shandong Provincial Key Laboratory of Network-Based Intelligent Computing, University of Jinan, Jinan 250022, China (e-mail: ise_hansy@ujn.edu.cn; ise_zhouj@ujn.edu.cn; yhchen@ujn.edu.cn; ise_wanglin@ujn.edu.cn).

Yi-Fan Zhang is with the CSIRO Agriculture and Food, Queensland Bioscience Precinct, St. Lucia, QLD 4067, Australia (e-mail: yi-fan.zhang@csiro.au).

Gong-You Tang is with the College of Information Science and Engineering, Ocean University of China, Qingdao 266100, China (e-mail: gtang@ouc.edu.cn).

Color versions of one or more of the figures in this article are available online at http://ieeexplore.ieee.org.

Digital Object Identifier 10.1109/TSMC.2020.2964607

In general, while diagnosing the fault signals by using the observer or filter technologies, the observer residual plays an important role by comparing with a preset threshold. For example, by constructing a filter with network packet indicator, an observer-based FD filter was designed by enhancing the ratio of fault sensitivity/disturbance attenuation and solving recursive Riccati equations in [28]; Su and Chen [26] proposed a model-based verification method for FD system by selecting a reasonable threshold so that the observer residuals and fault estimates could offset various noises, uncertainties, and variations; by integrating the time-varying gain bias faults into a general actuator fault model, a set of residuals for FD and isolation was built based on a proposed sliding-mode observer in [29]. The above FD methods provide the effective tools for detecting and isolating the fault signals. However, the complexities of the measurement equipment and the unsuitable threshold may bring out much difficult to diagnose the fault signals for real-time vehicle active suspension. Therefore, it is necessary to design a reduced-order observer independently of the observer residual for reducing the measurement cost and diagnosing the fault signals.

Besides, the FTC problem for vehicle active suspension attracts more and more attention to guarantee the reliability and improve the suspension performance [30], [31]. For example, considering the properties of nonlinearity and parameter uncertainties caused by suspension system itself and actuator fault, an adaptive robust controller was proposed to stabilize the vehicle active suspension based on accurate models exclusively in [32]; a realizable fuzzy H_∞ controller was derived for a T–S fuzzy active suspension system with actuator delays and faults in [33]; by designing an observer-based fault estimator with a generalized internal model control architecture, an $H\infty$ disturbance rejection controller for vehicle active suspension was designed for compensating actuator faults in [34]. The aforementioned FTC schemes are capable of compensating faults in actuator and/or measurement. In practice, comparing with the continuous-time vehicle active suspension [35], facilitating the collection and sharing of the suspension status is the advantages of vehicle active suspension under a digital control system and in-vehicle communication network, which becomes one of the primary tendency of the advanced vehicle active safety technology. Therefore, vehicle active suspension in the discrete-time domain could respond and compensate the faults rapidly while diagnosing the faults in actuator and/or measurement.

Motivated by the above analysis, this article focuses on the active FTC problem for vehicle active suspension, where the irregular road disturbances and the faults in actuator and measurement are taken into consideration. First, the vibration control problem for discrete vehicle active suspension is formulated to design an active fault-tolerant controller comprising of physically realizable optimal vibration control component and event-triggered fault-tolerant control component. After that, a physically realizable active fault-tolerant controller is proposed based on the designed reduced-order observer. Finally, experimental results demonstrate that the proposed approach has the capability of isolating the faults from suspension system states and real-time output, and guaranteeing good suspension performance under faults in actuator and measurement. In summary, the main contributions of this article are marked as follows.

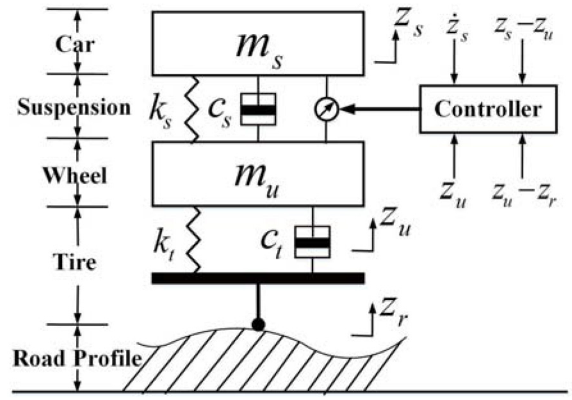

Fig. 1. Simple quarter vehicle active suspension.

1) By employing the real-time physical realizable output of vehicle active suspension rather than residual error, a reduced-order observer is proposed to estimate and diagnose the suspension system states and the fault states in actuator and measurement simultaneously, in which the poles of state equation of observer error are arranged to the unit circle of the Z plane by employing a reasonable feedback gain so that the asymptotic stability of observer error is guaranteed.
2) Based on the observed suspension system states and diagnosed fault states, a physical realizable active fault-tolerant controller is designed, in which an optimal vibration control component is designed to offset the vibration caused from road disturbances, and an event-triggered FTC component is constructed to compensate the faults in actuator and measurement.

The rest of this article is organized as follows. Section II describes the FTC problem for discrete vehicle active suspension. An active fault-tolerant controller via a reduced-order observer is designed in Section III. In Section IV, experimental results illustrate its superiority of the proposed fault-tolerant controller over other control schemes. Finally, Section V gives the findings of this article and some discussions for further work.

II. Problem Formulation

A. Discrete Model of Vehicle Active Suspension With Faults

Considering a simplified quarter vehicle active suspension displayed in Fig. 1, under an ideal actuator neglected the dynamic characteristics, the governing equations of the motion for the sprung and unsprung masses of vehicle active suspension are described as

$$\begin{cases} m_s\ddot{z}_s(t) + c_s[\dot{z}_s(t) - \dot{z}_u(t)] + k_s[z_s(t) - z_u(t)] = u(t) \\ m_u\ddot{z}_u(t) + c_s[\dot{z}_u(t) - \dot{z}_s(t)] + k_s[z_u(t) - z_s(t)] \\ \qquad + k_t[z_u(t) - z_r(t)] + c_t[\dot{z}_u(t) - \dot{z}_r(t)] = -u(t) \end{cases} \tag{1}$$

where m_s and z_s denote the mass and displacement of sprung components; z_s and z_u are the mass and displacement of unsprung components; k_t and c_t refer to the compressibility and damping of the pneumatic tire; and c_s and k_s stand for the damping and stiffness of vehicle suspension, respectively.

z_r represents the road irregularities and $u(t)$ is the control force generated from advanced actuator.

From the perspective of performance requirements, the sprung mass acceleration $\ddot{z}_s(t)$, the suspension deflection $z_s(t)-z_u(t)$, and tire deflection $z_u(t)-z_r(t)$ must be restricted to small values to improve the ride comfort, prevent the excessive suspension bottoming and provide the better road holding ability. Then the controlled output $y_c(t)$ and measurement output $y_m(t)$ are defined as

$$\begin{cases} y_c(t) = [\ddot{z}_s(t) \quad z_s(t) - z_u(t) \quad z_u(t) - z_r(t)]^T \\ y_m(t) = [z_s(t) - z_u(t) \quad \dot{z}_s(t)]^T. \end{cases} \tag{2}$$

The following state variables and the corresponding state vector $\bar{x}(t)$ are introduced as:

$$\begin{cases} x_1(t) = z_s(t) - z_u(t), \quad x_2(t) = z_u(t) - z_r(t), \\ x_3(t) = \dot{z}_s(t), \quad x_4(t) = \dot{z}_u(t) \\ \bar{x}(t) = [x_1(t) \ x_2(t) \ x_3(t) \ x_4(t)]^T \end{cases} \tag{3}$$

where $x_1(t)$ denotes the suspension deflection, $x_2(t)$ is the tire deflection, and $x_3(t)$ and $x_4(t)$ represent the velocities of the sprung mass and unsprung mass, respectively.

Then the normal continuous-time state space of vehicle active suspension without fault signals is described as

$$\begin{cases} \dot{\bar{x}}(t) = \bar{A}\bar{x}(t) + \bar{B}u(t) + \bar{D}_v v(t) \\ y_c(t) = C\bar{x}(t) + Eu(t) \\ y_m(t) = \bar{C}\bar{x}(t) \\ \bar{x}(0) = \bar{x}_0 \end{cases} \tag{4}$$

where $v(t) = \dot{z}_r(t)$, and

$$\bar{A} = \begin{bmatrix} 0 & 0 & 1 & -1 \\ 0 & 0 & 0 & 1 \\ -\frac{k_s}{m_s} & 0 & -\frac{c_s}{m_s} & \frac{c_s}{m_s} \\ \frac{k_s}{m_u} & -\frac{k_t}{m_u} & \frac{c_s}{m_u} & -\frac{(c_s+c_t)}{m_u} \end{bmatrix}$$

$$\bar{B} = \begin{bmatrix} 0 \\ 0 \\ \frac{1}{m_s} \\ -\frac{1}{m_u} \end{bmatrix}, \ \bar{D}_v = \begin{bmatrix} 0 \\ -1 \\ 0 \\ \frac{c_t}{m_u} \end{bmatrix}, E = \begin{bmatrix} \frac{1}{m_s} \\ 0 \\ 0 \end{bmatrix}$$

$$C = \begin{bmatrix} -\frac{k_s}{m_s} & 0 & -\frac{c_s}{m_s} & \frac{c_s}{m_s} \\ 1 & 0 & 0 & 0 \\ 0 & 1 & 0 & 0 \end{bmatrix}, \bar{C} = \begin{bmatrix} 1 & 0 & 0 & 0 \\ 0 & 0 & 1 & 0 \end{bmatrix}. \tag{5}$$

Setting the sampling period as T in the in-vehicle communication network, the normal form of vehicle active suspension (4) in the discrete-time domain is described as

$$\begin{cases} x(k+1) = Ax(k) + Bu(k) + D_v v(k) \\ y_c(k) = Cx(k) + Eu(k) \\ y_m(k) = \bar{C}x(k) \\ x(0) = x_0 \end{cases} \tag{6}$$

where $A = e^{\bar{A}T}, B = \int_0^T e^{\bar{A}t}\bar{B}dt$, and $D_v = \int_0^T e^{\bar{A}t}\bar{D}_v dt$.

Remark 1: Due to the limitation of measurement technologies and the physical structure aspects of vehicle suspension, it is uneconomical to measure all system variables. Especially, obtaining the values of tire deflection $x_2(k)$ and velocity $x_3(k)$ of unsprung mass is physically unrealizable or with huge cost. Thus, the designed measurement output $y_m(k)$ just includes the suspension deflection and the velocity of the sprung mass.

Remark 2. The measurement and control actions for vehicle active suspension (6) are clock-driven under sensors and in-vehicle communication network. Meanwhile, the measurement information is transmitted to the control center by the single packet with a time stamp.

Taking the faults in actuator and measurement into account, system (6) is rewritten as

$$\begin{cases} x(k+1) = Ax(k) + Bu(k) + D_v v(k) + D_a f(k) \\ y_c(k) = Cx(k) + Eu(k) + D_a f(k) \\ y_m(k) = \bar{C}x(k) + D_s f(k) \end{cases} \tag{7}$$

where $f(k) \in \mathbb{R}^m$ denotes directly unmeasurable fault signal vector; and D_a and D_s are the constant matrices of appropriate dimensions.

By employing an exosystem, the dynamic characteristics of fault signal vector $f(k)$ in the discrete-time domain are described as

$$\begin{cases} \varphi(k+1) = G_f \varphi(k), & k = k_0, k_0+1, k_0+2, \ldots \\ \varphi(k) = 0, & k = 0, 1, \ldots, k_0 - 1 \\ \varphi(k_0) = \varphi_{k_0} = \left[\varphi_a^T(\alpha) \ \ 0\right]^T, & \alpha = k_0 < \beta \\ \varphi(k_0) = \varphi_{k_0} = \left[0 \ \ \varphi_s^T(\beta)\right]^T, & k_0 = \beta < \alpha \\ f(k) = F_f \varphi(k), & k = 0, 1, 2, \ldots \end{cases} \tag{8}$$

where

$$\varphi(k) = \begin{bmatrix} \varphi_a(k) \\ \varphi_s(k) \end{bmatrix}, f(k) = \begin{bmatrix} f_a(k) \\ f_s(k) \end{bmatrix}$$
$$G_f = \begin{bmatrix} G_a & 0 \\ 0 & G_s \end{bmatrix}, F_f = \begin{bmatrix} F_a & 0 \\ 0 & F_s \end{bmatrix} \tag{9}$$

$\varphi_a(k) \in \mathbb{R}^{r_1}$ and $\varphi_s(k) \in \mathbb{R}^{r_2}$ denote the state vectors of actuator and measurement faults with $r = r_1 + r_2$, respectively; $\varphi(k) \in \mathbb{R}^r (m \leq r)$ denotes the fault state vector; $f_a(k) \in \mathbb{R}^{m_1}$ and $f_s(k) \in \mathbb{R}^{m_2}$ are the signal vectors of actuator and measurement faults with $m = m_1 + m_2$, respectively; α and β represent the initial unknown occurrence time of actuator and measurement faults; and $k_0 = \min\{\alpha, \beta\}$. While $k < \alpha$, $\varphi_a(k) = 0$. While $k < \beta$, $\varphi_s(k) = 0$. $G_f \in \mathbb{R}^{r \times r}$ and $F_f \in \mathbb{R}^{m \times r}$ are the real constant matrices, in which G_a, G_s, F_a, and F_s are with appropriate dimensions.

Remark 3: Model (8) can cover whether instant or constant/persistent faults in actuator and measurement with known characteristics and unknown magnitudes and phases [36], [37], such as step fault signal, sinusoidal fault signals, and other fault signals.

It could be pointed that the actual vehicle suspension structure without control input is stable but not asymptotically stable. The following assumptions, without loss of generality, are provided to design the fault-tolerant controller.

Assumption 1: The pair of $(\bar{A}, \bar{B})$ is completely controllable.

Assumption 2: The pairs of $(C, \bar{A})$ and (F_f, G_f) are completely observable.

B. Modeling of Road Disturbances

For the purpose of improving suspension performance, including ride comfort, road holding ability, and suspension deflection, external random road disturbances must be taken into account while constructing the vibration controller. Road disturbances are generally viewed as vibrations and specified as a random process involved with the following ground displacement PSD under different road roughnesses, which is described as:

$$G_d(\Omega) = \begin{cases} G_d(\Omega_0)(2\pi\Omega)^{-n_1}, & \Omega \leq \Omega_0 \\ G_d(\Omega_0)(2\pi\Omega)^{-n_2}, & \Omega > \Omega_0 \end{cases} \tag{10}$$

where Ω denotes a spatial frequency, and n_1 and n_2 are road roughness constants. The value of $G_d(\Omega_0)$ is determined by the estimation of road roughness. In particular, vehicle active suspension is extremely sensitive to road disturbances around its natural fixed frequency $\omega_n = \sqrt{k_s/m_s}$. Therefore, the considered frequency range of road disturbances is arranged in $[\omega_1, \omega_2] = [\beta_1\omega_n, \beta_2\omega_n]$ with $0 < \beta_1 < 1 < \beta_2$. Taken the low pass filtering characteristic of vehicle active suspension into account, the range of spatial frequency Ω sets as $[\omega_1/v_0, \omega_2/v_0]$ with vehicle constant velocity v_0.

Under the assumption that road irregularities approximate to the periodic function, based on the spectral representation method, road irregularities $z_r(t)$ can be computed from the following finite sum of Fourier series:

$$z_r(t) = \sum_{i=0}^{p-1} Z_i \sin\left[\left(\omega_1 + \frac{i2\pi v_0}{l}\right)t + \theta_i\right] \tag{11}$$

where $p \in [(\omega_2 - \omega_1)l/2\pi v_0 + 1, (\omega_2 - \omega_1)l/2\pi v_0 + 2)$ restricts the frequency of road irregularities, and $\theta_i \in [0, 2\pi)$ is a random variable. The amplitude Z_i in each harmonic component is given by

$$Z_i = \sqrt{\frac{4\pi G_d(\omega_1 l + 2\pi i v_0)}{v_0 l^2}} = \frac{0.2v_0\sqrt{l\pi G_d(\Omega_0)}}{l\omega_1 + 2\pi i v_0} \tag{12}$$

in which l is the road length. Then road disturbances $v(t)$ can be written as

$$\begin{aligned} v(t) &= \dot{z}_r(t) \\ &= 0.2v_0\sqrt{\frac{\pi G_d(\Omega_0)}{l}} \sum_{i=0}^{p-1} \cos\left[\left(\omega_1 + \frac{i2\pi v_0}{l}\right)t + \theta_i\right]. \end{aligned} \tag{13}$$

The following state vector $w(t)$ is introduced to obtain the state-space equation of road disturbances:

$$w(t) = \begin{bmatrix} w_1(t) & \cdots & w_{2p}(t) \end{bmatrix}^T \in \mathbb{R}^{2p}. \tag{14}$$

Then road disturbances $v(t)$ can be generated from the following exosystem:

$$\begin{cases} \dot{w}(t) = \bar{G}_v w(t) \\ v(t) = F_v w(t) \end{cases} \tag{15}$$

where $\bar{G}_v \in \mathbb{R}^{2p \times 2p}$, $F_v \in \mathbb{R}^{1 \times 2p}$, and

$$\begin{aligned} \bar{G}_v &= \begin{bmatrix} \mathbf{0} & \mathbf{I} \\ \tilde{G} & \mathbf{0} \end{bmatrix} \\ F_v &= \begin{bmatrix} \underbrace{0, \ldots, 0,}_{p} \underbrace{1, \ldots, 1}_{p} \end{bmatrix} \\ \tilde{G} &= \operatorname{diag}\left\{ -\omega_1^2, \ \ldots, -\left(\omega_1 + (p-1)\frac{2\pi v_0}{l}\right) \right\}. \end{aligned} \tag{16}$$

Noting that $\operatorname{rank}[F^T, (F\bar{G}_v)^T, \ldots, (F\bar{G}_v^{2p-1})^T]^T = 2p$, the pair of $(F_v, \bar{G}_v)$ is completely observable.

With the sampling period T, (15) in the discrete-time domain is formulated as

$$\begin{cases} w(k+1) = G_v w(k) \\ v(k) = F_v w(k) \end{cases} \tag{17}$$

where $G_v = e^{\bar{G}_v T}$.

C. Problem Description

In order to satisfy the performance requirements and ensure the safety of vehicle active suspension, the controller structure comprised of vibration component and fault-tolerant component is introduced first

$$u(k) = \begin{cases} u_c(k), & f_a(k) = 0 \\ u_c(k) + u_f(k), & f_a(k) \neq 0 \end{cases} \tag{18}$$

where $u_c(k)$ denotes the optimal vibration control component to offset the vibration, and $u_f(k)$ represents the FTC component to compensate the faults in actuator and measurement.

In the sense of optimal controller design, the optimal vibration control component $u_c(k)$ could be designed to minimize the following average quadratic performance index under the constraints of (8) and (17) with small energy consumption:

$$J = \lim_{N\to\infty} \frac{1}{N} \sum_{k=0}^{N} \left[y_c^T(k) Q y_c(k) + u^T(k) R u(k) \right]. \tag{19}$$

However, optimal control component $u_c(k)$ is usually involved with the physically unrealizable feedback component of $x(k)$.

Meanwhile, while the faults occur in actuator or/and measurement, the FTC component $u_f(k)$ could be event-triggered timely and the system output could be restructured based on the actual system output. In general, the event-triggered FTC component $u_f(k)$ can be designed as

$$u_f(k) = -Mf(t) \tag{20}$$

which is under the assumption that $\operatorname{rank}(B) = \operatorname{rank}([\,B \ \ D_a\,])$. Under this assumption, it ensures that the actuator fault only occurs in actuator and directly affects the control input $u(k)$. Then the event-triggered FTC component $u_f(k)$ is physical realization.

Meanwhile, the event-triggered restructured system output could be designed as

$$\bar{y}_m(k) = y_m(k) - D_s f(k). \tag{21}$$

It is obvious that the structures of FTC component (20) and restructured system output (21) depend on the fault signal $f(k)$. However, it is difficult to diagnose the fault signal $f(k)$ in actuator and measurement timely and accurately under irregular road disturbances.

Therefore, the FTC problem for vehicle active suspension with faults in actuator and measurement in the discrete domain is described as follows.

1) A physically realizable optimal vibration control component could be designed under the constraints of (6) and (17) with respect to performance index (19) thereby

the performance requirements of discrete vehicle active suspension can be satisfied effectively.

2) A reduced-order observer could be designed to estimate the system state $x(k)$ and diagnose the fault signal $f(k)$. Thus, the event-triggered FTC component (20) and the restructured system output (21) can be physical realizable and activated to compensate the faults. Meanwhile, the physical realizable problem for optimal vibration control component $u_c(k)$ can be resolved.

III. Active Fault-Tolerant Controller via Reduced-Order Observer

In this section, an augmented system is designed first by combining the system states of discrete vehicle active suspension (7) and fault signals (8). Then an active fault-tolerant controller is proposed based on the optimal control theory via a reduced-order observer.

Defining vector $z(k) = \begin{bmatrix} x^T(k) & \varphi^T(k) \end{bmatrix}^T$ and combining systems of (7) and (8), the following augmented system is obtained as:

$$\begin{cases} z(k+1) = A_z(k) + B_z u(k) + D_z v(k) \\ y_c(k) = C_c z(k) + E_c u(k) \\ y_m(k) = C_m z(k) \end{cases} \tag{22}$$

where

$$\begin{aligned} A_z &= \begin{bmatrix} A & \begin{bmatrix} D_a F_f & 0 \end{bmatrix} \\ 0 & G_f \end{bmatrix}, \ B_z = \begin{bmatrix} B \\ 0 \end{bmatrix} \\ D_z &= \begin{bmatrix} D_v \\ 0 \end{bmatrix}, \ C_c = \begin{bmatrix} C & \begin{bmatrix} D_a F_f & 0 \end{bmatrix} \end{bmatrix} \\ E_c &= \begin{bmatrix} E \\ 0 \end{bmatrix}, \ C_m = \begin{bmatrix} \bar{C} & \begin{bmatrix} 0 & D_s F_f \end{bmatrix} \end{bmatrix}. \end{aligned} \tag{23}$$

Introducing the orthogonal complement matrix $C_{m\perp}^T$ for C_m, a nonsingular matrix H is constructed as

$$H = \begin{bmatrix} C_{m\perp}^T \\ C_m \end{bmatrix} \in \mathbb{R}^{(4+r)\times(4+r)} \tag{24}$$

where $C_m C_{m\perp}^T = 0$. Meanwhile, the structure of inverse matrix T of nonsingular matrix H is described as

$$T = H^{-1} = \begin{bmatrix} T_1 & T_2 \end{bmatrix} = \begin{bmatrix} T_{11} & T_{12} \\ T_{21} & T_{22} \end{bmatrix} \tag{25}$$

where $T_1 \in \mathbb{R}^{(4+r)\times(2+r)}$, $T_2 \in \mathbb{R}^{(4+r)\times 2}$, $T_{11} \in \mathbb{R}^{4\times(2+r)}$, $T_{12} \in \mathbb{R}^{4\times 2}$, $T_{21} \in \mathbb{R}^{r\times(2+r)}$, and $T_{22} \in \mathbb{R}^{r\times 2}$.

In order to describe the main result more clearly, the following matrices are introduced as:

$$\begin{aligned} \tilde{R} &= E^T Q E + R, \ A_1 = A - B\tilde{R}^{-1}E^T QC \\ Q_1 &= C^T QC - C^T QE\tilde{R}^{-1}E^T QC. \end{aligned} \tag{26}$$

Then the active fault-tolerant controller is given in the following theorem via a designed reduced-order observer.

Theorem 1: Consider the discrete vehicle active suspension (7) subject to persistent road disturbances (17) and faults (8) in actuator and measurement, a reduced-order observer is constructed to estimate the system state $x(k)$ and diagnose the fault state $\varphi(k)$, which is formulated as

$$\begin{cases} \hat{z}_o(k+1) = \left(C_{m\perp}^T - LC_m\right)\left\{A_z T_1 \hat{z}_o(k) \right. \\ \qquad \left. + A_z(T_1 L + T_2)y_m(k) + B_z u(k) + D_z v(k)\right\} \\ \hat{x}(k) = T_{11}\hat{z}_o(k) + (T_{11}L + T_{12})y_m(k) \\ \hat{\varphi}(k) = T_{21}\hat{z}_o(k) + (T_{21}L + T_{22})y_m(k) \end{cases} \tag{27}$$

where $\hat{z}_o(k) \in \mathbb{R}^{(2+r)\times 2}$ denotes the observer state, $\hat{x}(k)$ and $\hat{\varphi}(k)$ are the estimation values of discrete vehicle active suspension state $x(k)$ in (7) and fault state $\varphi(k)$ in (8), respectively. $L \in \mathbb{R}^{(2+r)\times 2}$ denotes a reasonable feedback gain to arrange the poles of the matrix $((C_{m\perp}^T - LC_m)A_z T_1)$ to the unit circle of the Z plane.

Then, the active fault-tolerant controller $u(k)$ is proposed, which is given by

$$u(k) = \begin{cases} u_c(k), & f(k) = 0 \\ u_c(k) + u_f(k), & f(k) \neq 0 \end{cases} \tag{28}$$

where $u_c(k)$ denotes the physical realizable optimal vibration control component for offsetting the road disturbances, which is given by

$$\begin{aligned} u_c(k) = -\tilde{R}^{-1}\Big\{&\Big(E^T QC + B^T A_1^{-T}(P_1 - Q_1)\Big) \\ &\times \big(T_{11}\hat{z}_o(k) + (T_{11}L + T_{12})y_m(k)\big) \\ &+ B^T A_1^{-T} P_2 w(k)\Big\} \end{aligned} \tag{29}$$

in which P_1 is the unique positive definite solution of the following Riccati matrix equation:

$$P_1 = Q_1 + A_1^T P_1 S^{-1} A_1 \tag{30}$$

and P_2 is the unique solution of the following Stein matrix equation:

$$\begin{aligned} P_2 = &A_1^T P_1 S^{-1} D_v F_v \\ &+ A_1^T\Big(I - P_1 S^{-1} B\tilde{R}^{-1}B^T\Big)P_2 G_v \end{aligned} \tag{31}$$

with $S = I + B\tilde{R}^{-1}B^T P_1$.

Meanwhile, $u_f(k)$ is the event-triggered FTC component for compensating the faults in actuator and measurement, which is designed as

$$u_f(k) = -MF_f\big(T_{21}\hat{z}_o(k) + (T_{21}L + T_{22})\bar{y}_m(k)\big) \tag{32}$$

the event-triggered restructured system output $\bar{y}_m(k)$ for isolating the fault signals in measurement from system output is introduced as

$$\bar{y}_m(k) = \begin{cases} y_m(k), & f_s(k) = 0 \\ y_m(k) - D_S F_f \times (T_{21}\hat{z}_o(k) & \\ \quad + (T_{21}L + T_{22})y_m(k)), & f_s(k) \neq 0. \end{cases} \tag{33}$$

Proof: Taking no account of faults in actuator and measurement, a physically unrealizable optimal vibration control component is designed first.

Applying the typical optimal control theory, the optimal vibration control component can be obtained concerning the performance index (19), which is given by

$$u_c(k) = -\tilde{R}^{-1}\big[E^T QCx(k) + B^T\lambda(k+1)\big] \tag{34}$$

where $\lambda(k)$ can be obtained from the following two-point boundary value (TPBV) problem:

$$\begin{cases} x(k+1) = A_1 x(k) \\ \quad -B\tilde{R}^{-1}B^T\lambda(k+1) + D_v F_v w(k) \\ \lambda(k) = Q_1 x(k) + A_1^T \lambda(k+1) \\ x(0) = x_0, \quad \lambda(\infty) = 0. \end{cases} \tag{35}$$

Defining $\lambda(k) = P_1 x(k) + P_2 w(k)$, (35) is reformulated as

$$\begin{cases} \lambda(k+1) = A_1^{-T}[(P_1 - Q_1)x(k) + P_2 w(k)] \\ x(k+1) = S^{-1} \\ \quad \times \big(A_1 x(k) + \big(D_v F_v - B\tilde{R}^{-1}B^T P_2 G_v\big)w(k)\big) \\ \lambda(\infty) = 0, \quad x(0) = x_0. \end{cases} \tag{36}$$

Then the optimal vibration control component $u_c(k)$ is formulated as

$$u_c(k) = -\tilde{R}^{-1}\Big(\Big(E^T QC + B^T A_1^{-T}(P_1 - Q_1)\Big)x(k) + B^T A_1^{-T} P_2 w(k)\Big). \tag{37}$$

Rearranging (35)–(37), one gets

$$\begin{aligned} \lambda(k) &= Q_1 x(k) + A_1^T \lambda(k+1) \\ &= \Big(Q_1 + A_1^T P_1 S^{-1} A_1\Big)x(k) \\ &\quad + \Big(A_1^T P_2 G_v + A_1^T P_1 S^{-1}\Big(D_v F_v - B\tilde{R}^{-1}B^T P_2 G_v\Big)\Big)w(k). \end{aligned} \tag{38}$$

Noting the parameters of (38), Riccati matrix equation (30) and Stein matrix equation (31) can be obtained. Because the pair of (A, B, C) is completely controllable and observable, P_1 is the unique solution of Riccati equation (30). Meanwhile, based on the second formula of (36), we have

$$\begin{cases} \big|\sigma_i\big(S^{-1}A_1\big)\big|\big|\sigma_j(G_v)\big| < 1 \\ i = 1, 2, \ldots, 4 + r; \quad j = 1, 2, \ldots, l \end{cases} \tag{39}$$

where $\sigma(\cdot)$ denotes the eigenvalues of the matrix. Therefore, P_2 is the unique solution of Stein matrix equation (31). Because of the existence and uniqueness of P_1 and P_2, the stability of vehicle active suspension (7) can be guaranteed based on the Liapunov's stability criterion while the faults in actuator and measurement do not occur.

In addition, while the faults in actuator and measurement occur, the stability of vehicle active suspension could be guaranteed by isolating the fault signal $f(k)$ from the system sate $x(k)$ and the system output $y_m(k)$. Besides, focusing on the proposed optimal vibration controller (37), the precise values of all necessary status $x(k)$ are difficult to be estimated. In what is follows, a reduced-order observer will be proposed to design the event-triggered FTC component, restructure the system output, and make the optimal vibration component (37) physically realizable. Thus, the discrete vehicle suspension state $x(k)$ and fault state $\varphi(k)$ can be estimated.

Defining $\varpi(k) = Hz(k) = [\,\varsigma^T(k) \quad y_m(k)\,]$, one gets $z(k) = T_1\varsigma(k) + T_2 y_m(k)$. Then we have

$$\begin{cases} \varsigma(k+1) = C_{m\perp}^T(A_z T_1 \varsigma(k) \\ \quad + A_z T_2 y_m(k) + B_z u(k) + D_z v(k)) \\ y_m(k+1) = C_m(A_z T_1 \varsigma(k) \\ \quad + A_z T_2 y_m(k)) + B_z u(k) + D_z v(k)\big). \end{cases} \tag{40}$$

Introducing $z_o(k) = \varsigma(k) - L y_m(k)$ with the feedback gain matrix L, one gets

$$\begin{cases} z_o(k+1) = \big(C_{m\perp}^T - LC_m\big)(B_z u(k) + D_z v(k)) \\ \quad + \big(C_{m\perp}^T - LC_m\big)(A_z T_1 z_o(k) + A_z(T_1 L + T_2)y_m(k)) \\ z(k) = T_1 z_o(k) + (T_1 L + T_2)y_m(k). \end{cases} \tag{41}$$

Then a reduced-order observer is formulated as

$$\begin{cases} \hat{z}_o(k+1) = \big(C_{m\perp}^T - LC_m\big)(B_z u(k) + D_z v(k)) \\ \quad + \big(C_{m\perp}^T - LC_m\big)\big(A_z T_1 \hat{z}_o(k) + A_z(T_1 L + T_2)y_m(k)\big) \\ \hat{z}(k) = T_1 \hat{z}_o(k) + (T_1 L + T_2)y_m(k) \end{cases} \tag{42}$$

where $\hat{z}_o(k)$ denotes the observer state and $\hat{z}(k)$ is the estimated value of $z(k)$ in (22).

The observer error is given by

$$e(k) = z_o(k) - \hat{z}_o(k). \tag{43}$$

Based on (41) and (42), one gets

$$e(k+1) = \big(C_{m\perp}^T - LC_m\big)A_z T_1 e(k). \tag{44}$$

Noting that the pair of (C_m, A_z) is completely observable and $T_1 C_{m\perp}^T = I$, we have

$$\operatorname{rank}\begin{bmatrix} C_m A_z T_1 \\ C_m A_z T_1 C_{m\perp}^T A_z T_1 \\ \vdots \\ C_m A_z T_1\big(C_{m\perp}^T A_z T_1\big)^{n+r-q-1} \end{bmatrix} = \operatorname{rank}\begin{bmatrix} C_m A_z T_1 \\ C_m A_z^2 T_1 \\ \vdots \\ C_m A_z^{n+r-q-1} T_1 \end{bmatrix} = n + r - q. \tag{45}$$

Therefore, the pair of $(C_m A_z T_1, C_{m\perp}^T A_z T_1)$ is observable. It means that there exist a feedback gain L to arrange all eigenvalues of matrix $((C_{m\perp}^T - LC_m)A_z T_1)$ to the unit circle of the Z plane. Thus, observer error $e(k)$ in (44) is asymptotic stability and one has

$$\lim_{k\to\infty} \hat{z}(k) = z(k). \tag{46}$$

Based on the second formula in (42), the estimation values $\hat{x}(k)$ and $\hat{\varphi}(k)$ for discrete vehicle suspension state $x(k)$ and fault state $\varphi(k)$ are formulated as

$$\begin{cases} \hat{x}(k) = T_{11}\hat{z}_o(k) + (T_{11}L + T_{12})y_m(k) \\ \hat{\varphi}(k) = T_{21}\hat{z}_o(k) + (T_{21}L + T_{22})y_m(k). \end{cases} \tag{47}$$

From (44) and (47), we have

$$\begin{cases} \lim\limits_{k\to\infty}\big(\hat{x}(k) - x(k)\big) = 0 \\ \lim\limits_{k\to\infty}\Big(\hat{f}(k) - f(k)\Big) = \lim\limits_{k\to\infty}\big(F_f\hat{\varphi}(k) - F_f\varphi(k)\big) = 0. \end{cases} \tag{48}$$

The matrix L in (44) could be chosen reasonably so that observer error $e(k)$ can be converged quicker than that of vehicle active suspension. Then vehicle active suspension (7) is rewritten as

$$\begin{cases} x(k+1) = Ax(k) + Bu_c(k) + BM\Big(f(k) - \hat{f}(k)\Big) + D_v v(k) \\ y_m(k) = \bar{C}x(k) + D_s\Big(f(k) - \hat{f}(k)\Big). \end{cases} \tag{49}$$

TABLE I
THREE SCENARIOS UNDER DIFFERENT ROAD ROUGHNESSES, ROAD LENGTHS, AND VEHICLE VELOCITIES

Scenarios	Scenario 1	Scenario 2	Scenario 3
Road roughness (m^3)	64×10^{-6}	256×10^{-6}	1024×10^{-6}
Road profile grade	C grade	D grade	E grade
Road surface condition	Average	Poor	Very poor
Road length (m)	320	450	450
Vehicle velocity (m/s)	20	25	30

By integrating the first formula in (49) based on (37) and (47), we have

$$\begin{cases} x(k+1) = Ax(k) + BM\Big(f(k) - \hat{f}(k)\Big) \\ \quad + \Big(D_v F_v - B\tilde{R}^{-1}B^T A_1^{-T} P_1\Big)w(k) \\ \quad - B\tilde{R}^{-1}\Big(E^T QC + B^T A_1^{-T}(P_1 - Q_1)\Big)\hat{x}(k) \\ y_m(k) = \bar{C}x(k) + D_s(f(k) - \hat{f}(k)). \end{cases} \tag{50}$$

Based on (48), along with $k \to \infty$, the fault signal $f(k)$ is isolated from the system sate $x(k)$ and the system output $y_m(k)$. Therefore, the stability properties of vehicle active suspension can be guaranteed.

Integrating (47) and the first formula in (42), the reduced-order observer (27) is obtained. Meanwhile, by substituting the estimation values $\hat{x}(k)$ to the optimal vibration control component (37), the physically realizable optimal vibration control component (29) is designed. By substituting the estimation values $\hat{\varphi}(k)$ into (20) and (21), the event-triggered FTC component (32) and restructured system output (33) are obtained. The proof is completed. ■

Remark 4: Noting the proposed event-triggered FTC component (32) and restructured system output (33), the FTC component will be event-triggered to compensate the fault in actuator and measurement while diagnosing the fault signal $f_a(k) \neq 0$ or $f_s(k) \neq 0$.

IV. EXPERIMENTAL RESULTS

In this section, the proposed active FTC scheme is applied on a quarter discrete vehicle active suspension. The experimental results will be thoroughly analyzed to demonstrate the effectiveness of the designed reduced-order observer (27) and the proposed active fault-tolerant controller (28).

The parameters of vehicle active suspension are listed as follows [35]: the sprung mass m_s and unsprung mass m_u are 9527.6 N and 1113.3 N; the damping c_s and stiffness k_s of the passive suspension system are 1095 Ns/m and 42719.6 N/m; and the compressibility k_t and damping c_t of the pneumatic tire set as 101115 N/m and 14.6 Ns/m. Based on these parameters, the matrices A, B, D_v, C, and E in (7) are obtained under the sampling period $T = 0.08$ s.

Meanwhile, the road displacement input is generated from exosystem (17), where $w_n = 2.1175$, $\beta_1 = 0.5$, and $\beta_2 = 5$. In order to cover more scenarios about simulation conditions, three scenarios are selected under different road roughnesses, road lengths, and vehicle velocities, which are listed in Table I. More especially, considering the Scenario 2 with $v_0 = 25$ m/s

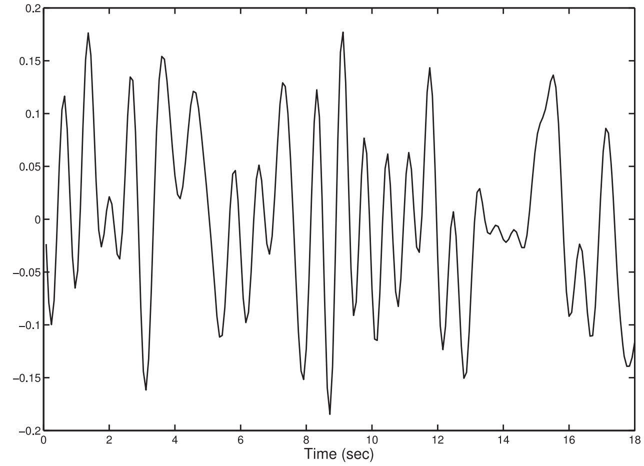

Fig. 2. Curve of random road disturbances.

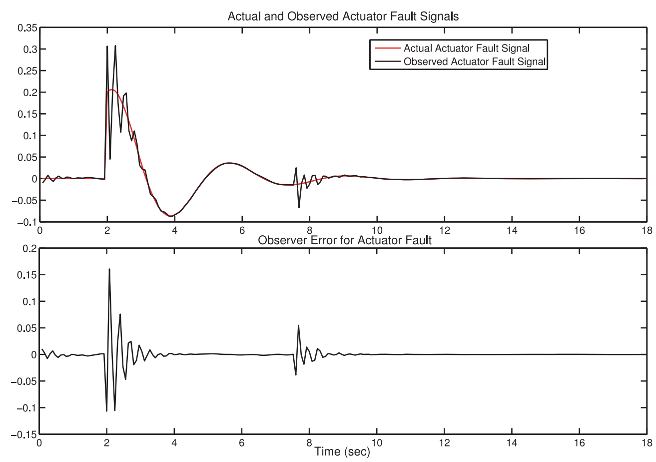

Fig. 3. Curves of observer error, actual, and observed signals of actuator fault.

and $l = 450$ m, the road disturbance $v(k)$ is computed and depicted in Fig. 2.

A. Performance of Diagnosing the Faults in Actuator and Measurement

Two different kinds of faults are considered, in which the instant actuator fault occurs at 2 s and the persistent measurement fault occurs at 7.6 s, respectively. Meanwhile, based on the proposed Theorem 1, the feedback gain L is chosen reasonably for the reduced-order observer (27) to assign the poles of matrix $((C_{m\perp}^T - LC_m)A_z T_1)$ to $0.4 \pm 0.2j$, $0.3 \pm 0.03j$ and $0.1 \pm 0.01j$, which is given by

$$L = \begin{bmatrix} 110.5 & 20.5 & 205.7 & -76.1 & 88.5 & -16.7 \\ 96.1 & 24.2 & 229.7 & -74.6 & 101.5 & -3.5 \end{bmatrix}^T. \tag{51}$$

In order to show the authenticity of the observers convergence, the curves of actual and observed fault signals in actuator and measurement, and observer errors are displayed in Figs. 3 and 4. It is obvious that, whether the persistent/constant fault signal or the instant fault signal, the proposed reduced-order observer could diagnose the faults signals while occurring the actual faults simultaneously, and make the convergence to zero of the observer errors for faults in

This article has been accepted for inclusion in a future issue of this journal. Content is final as presented, with the exception of pagination.

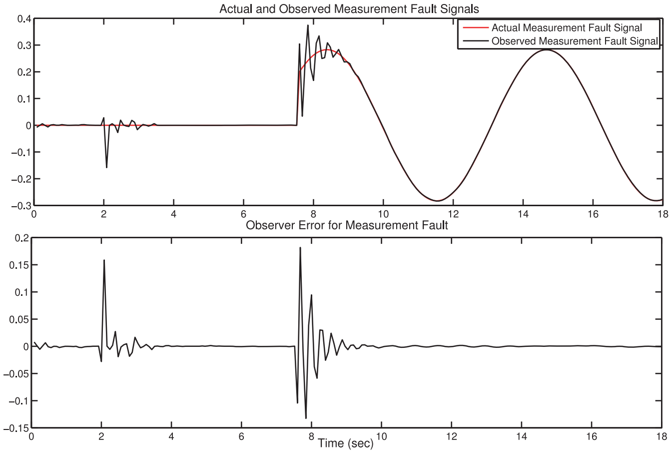

Fig. 4. Curves of observer error, actual, and observed signals of measurement fault.

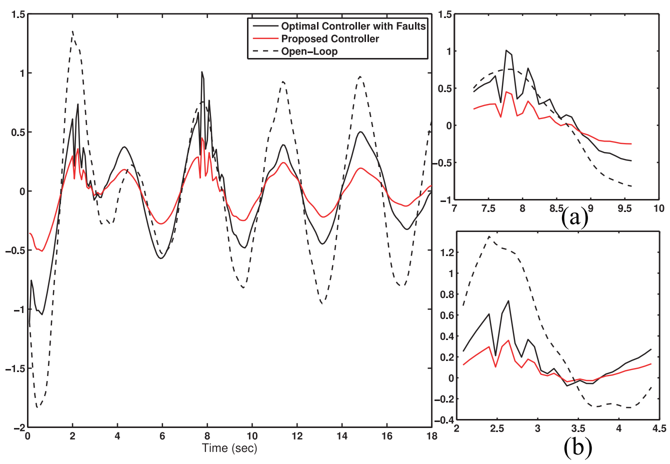

Fig. 5. Comparison curves of sprung mass acceleration under different control schemes.

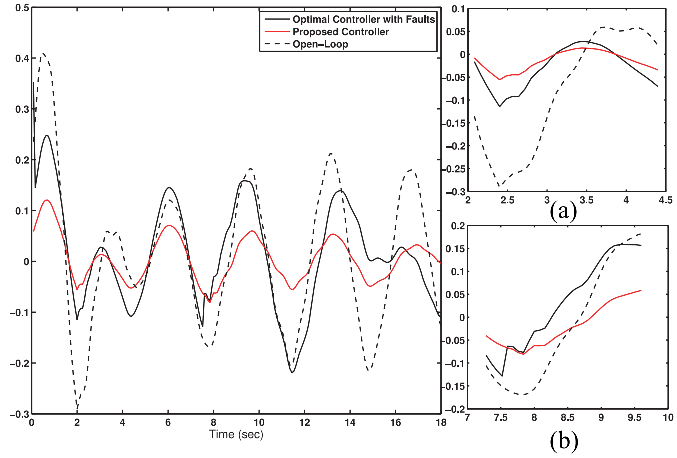

Fig. 6. Comparison curves of suspension deflection under different control schemes.

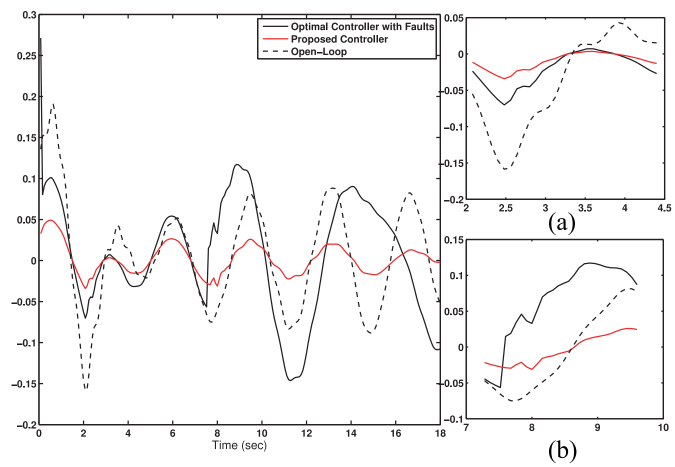

Fig. 7. Comparison curves of tire deflection under different control schemes.

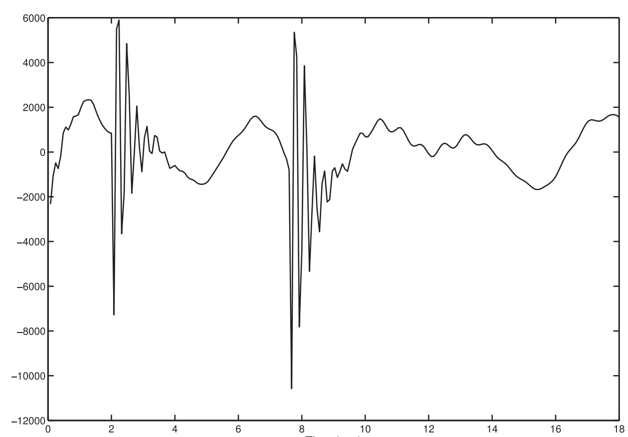

Fig. 8. Curve of proposed active FTC law.

actuator and measurement. Meanwhile, noting the curve of observed actuator fault signal at 2 s and the curve of observed measurement fault signal at 7.6 s, short-term oscillations are occurred. Those are triggered by the interplay between the actuator fault and the measurement fault. Besides, the observer errors in the beginning phase are caused by the initial state of vehicle active suspension.

Then the validity of the proposed reduced-order observer (27) is illustrated for estimating the fault signals. Therefore, the proposed active fault-tolerant controller (28) can be realized.

B. Effectiveness of the Proposed Vehicle Active Fault-Tolerant Controller

Considering three different conditions under Scenario 2 in Table I, including vehicle active suspension (7) with faults under the optimal vibration control component (37), vehicle active suspension (7) with faults under the active fault-tolerant controller (28) via reduced-order observer (27), and the open-loop vehicle active suspension, the comparison curves of the sprung mass acceleration $\ddot{z}_s$, the suspension deflection $z_s - z_u$, and the tire deflection $z_u - z_r$ are shown in Figs. 5–7, respectively, where the transient responses for actuator fault and measurement fault are displayed. The curve of the proposed active fault-tolerant controller (28) is displayed in Fig. 8.

From Figs. 5–7, it can be noted that the basic performance requirements under the proposed FTC scheme (28) can be arranged to smaller values than ones under open-loop vehicle suspension, and ones of vehicle active suspension with faults under the optimal vibration control component (37).

TABLE II
RMS VALUES OF SPRUNG MASS ACCELERATION (m/s^2) UNDER DIFFERENT ROAD ROUGHNESSES, VEHICLE VELOCITIES, AND ROAD LENGTHS

Different simulation scenarios	Scenario 1	Scenario 2	Scenario 3
Uncontrolled case	0.33	0.69	1.33
$H\infty$ controller in [35] without faults and delays	0.18 (-45.45%)	**0.36 (-47.82%)**	0.72 (-45.86%)
Optimal controller (37) with faults	0.26 (-21.21%)	0.51 (-26.08%)	1.11 (-16.54%)
Proposed controller (28) with faults	**0.16 (-51.51%)**	0.38 (-44.93%)	**0.45 (-66.16%)**

TABLE III
RMS VALUES OF SUSPENSION DEFLECTION (cm) UNDER DIFFERENT ROAD ROUGHNESSES, VEHICLE VELOCITIES, AND ROAD LENGTHS

Different simulation scenarios	Scenario 1	Scenario 2	Scenario 3
Uncontrolled case	0.69	1.48	2.81
$H\infty$ controller in [35] without faults and delays	**0.49 (-28.98%)**	0.98 (-33.78%)	1.96 (-30.25%)
Optimal controller (37) with faults	0.65 (-5.797%)	1.42 (-4.054%)	2.85 (-1.423%)
Proposed controller (28) with faults	0.50(-27.53%)	**0.76(-48.64%)**	**1.28(-54.45%)**

TABLE IV
RMS VALUES OF TIRE DEFLECTION (cm) UNDER DIFFERENT ROAD ROUGHNESSES, VEHICLE VELOCITIES, AND ROAD LENGTHS

Different simulation scenarios	Scenario 1	Scenario 2	Scenario 3
Uncontrolled case	0.43	0.90	1.75
$H\infty$ controller in [35] without faults and delays	0.36 (-16.28%)	0.71 (-21.11%)	1.42 (-18.86%)
Optimal controller (37) with faults	0.33 (-23.26%)	1.06 (+117.8%)	1.65 (-5.714%)
Proposed controller (28) with faults	**0.29 (-32.56%)**	**0.28 (-68.89%)**	**0.65 (-62.85%)**

Meanwhile, by observing Fig. 8, the proposed active fault-tolerant controller (28) can provide a quick response while the faults in actuator and measurement occur, in which an ideal actuator neglecting the dynamic characteristics is employed to generate the control forces.

More especially, for the open-loop case, vehicle active suspension without control input can be stable but not asymptotically stable caused by the damping k_t and stiffness c_s of passive vehicle suspension, which is in accordance with the statement above the Assumption 1. For vehicle active suspension with faults under the proposed FTC component (28), the related curves in Figs. 5–8 are sharper and more sudden while occurring the faults at $t = 0$ s, $t = 2$ s, and $t = 7.6$ s. As time goes on, the curves of suspension performance become smooth rapidly under the proposed FTC component (28) after diagnosing the faults in actuator and measurement. Meanwhile, noting vehicle active suspension with faults under the optimal vibration control component (37), the corresponding values and curves are larger and sharper than those of suspension with faults under the proposed fault-tolerant controller (28). It indicates that the optimal vibration control component (37) cannot compensate the occurred faults. Correspondingly, it is evident that the faults in actuator and measurement can be compensated effectively under the proposed fault-tolerant controller (28) while diagnosing the fault signals.

From the perspective of the quantitative values, the comparison results of root mean square (RMS) values of the sprung mass acceleration, suspension deflection, and tire deflection are listed in Table II–IV under different scenarios, where the open-loop case and simulation results from continuous-time vehicle active suspension in [35] without faults and delays are compared with experimental results of those under the proposed fault-tolerant controller (28) and the optimal vibration control component (37). Meanwhile, the percentage number given in the parentheses indicates the reduced amount of the closed-loop responses relative to the open-loop case. The bold data are the smallest value under the different control schemes in the same scenario.

For example, under Scenario 2 with road roughness $256 \times 10^{-6}\text{m}^3$, road length 450 m, and vehicle velocity 25 m/s, for vehicle active suspension with faults under the proposed fault-tolerant controller (28), RMS values of the sprung mass acceleration $\ddot{z}_s$, the suspension deflection $z_s - z_u$, and the tire deflection $z_u - z_r$ are reduced by about 44.93%, 48.64%, and 68.98% compared with those of the open-loop vehicle suspension. For continuous-time vehicle active suspension under $H\infty$ controller in [35] without faults and delays, RMS value of the sprung mass acceleration $\ddot{z}_s$, the suspension deflection $z_s - z_u$, and the tire deflection $z_u - z_r$ are reduced by about 47.82%, 33.78%, and 21.11% compared with those of the open-loop vehicle suspension. Relatively, under the optimal vibration control component (37), RMS values of the sprung mass acceleration $\ddot{z}_s$, the suspension deflection $z_s - z_u$, and the tire deflection $z_u - z_r$ are reduced by about 26.08%, 4.054%, and 117.8% compared with those of the open-loop vehicle suspension, respectively. For sprung mass acceleration, the smallest RMS value is under $H\infty$ controller in [35] without faults and delays. For suspension deflection and tire deflection, the smallest RMS values are under the proposed fault-tolerant controller (28). It can be observed that, compared with continuous-time vehicle active suspension under $H\infty$ controller in [35] without faults and delays, the proposed fault-tolerant controller (28) outperform slightly for reducing the sprung mass acceleration and suspension deflection. For reducing the tire deflection, the proposed fault-tolerant controller (28) behaves better.

By displaying and discussing the above experimental results, it can be concluded that the system states of vehicle active suspension and faults can be diagnosed precisely by using the designed reduced-order observer (27). Then the physically unrealizable problems for optimal vibration control component and event-triggered FTC component are resolved. Meanwhile, by applying the proposed active fault-tolerant controller (28) to discrete vehicle active suspension, the values of the sprung mass acceleration, suspension deflection, and tire deflection can be reduced to small values. Thus, the performances requirements are satisfied and the suspension performances are improved effectively.

V. Conclusion

An active fault-tolerant controller was proposed for a discrete vehicle active suspension with faults in actuator and measurement, which makes up a physical realizable optimal vibration control component and an event-triggered FTC component. Especially, a reduced-order observer was proposed by using the real-time output of vehicle active suspension to observe the suspension system state and diagnose the fault signals in actuator and measurement. Then an event-triggered FTC component and a restructured system output were obtained.

The main results in this article are under the assumptions that the normal model of vehicle active suspension is ideal formulated as a linear system with an ideal actuator, the dynamic of faults is with known characteristics, and the road roughnesses are with known values. On the contrary, vehicle active suspension is a complicated nonlinear system with delays and faults in actuator and measurement in practical systems. Meanwhile, active actuators usually have physical limitations. The designed control value cannot be more than fully open or fully closed. In addition, road roughnesses are varying over time, and the fault information usually is not fully accurate. Therefore, our future work will focus on the following three aspects.

1) The complicated active suspensions will be considered to improve the suspension performance, for example, the characteristics of uncertainties, nonlinearity, and delays and faults in actuator and measurement can be considered simultaneously.
2) We will consider the saturation dynamic characteristics of the actual actuator and discuss the anti-windup control problem for vehicle active suspension.
3) The road recognition problem and fault recognition problem will be discussed based on evolutionary computation theories so that the accurate information could be provided for designing the reasonable vibration and fault-tolerant controller.

References

[1] H. E. Tseng and D. Hrovat, "State of the art survey: Active and semi-active suspension control," *Veh. Syst. Dyn.*, vol. 53, no. 7, pp. 1034–1062, May 2015.

[2] M.-M. Ma and H. Chen, "Disturbance attenuation control of active suspension with nonlinear actuator dynamics," *IET Control Theory Appl.*, vol. 5, no. 1, pp. 112–122, Jan. 2011.

[3] W. Sun, H. Pan, Y. Zhang, and H. Gao, "Multi-objective control for uncertain nonlinear active suspension systems," *Mechatronics*, vol. 24, no. 4, pp. 318–327, Jun. 2014.

[4] P. Brezas and M. C. Smith, "Linear quadratic optimal and risk-sensitive control for vehicle active suspensions," *IEEE Trans. Control Syst. Technol.*, vol. 22, no. 2, pp. 543–566, Feb. 2014.

[5] S.-Y. Han, C.-H. Zhang, and G.-Y. Tang, "Approximation optimal vibration for networked nonlinear vehicle active suspension with actuator time delay," *Asian J. Control*, vol. 19, no. 3, pp. 983–995, May 2017.

[6] Y. Jin and X. Luo, "Stochastic optimal active control of a half-car nonlinear suspension under random road excitation," *Nonlin. Dyn.*, vol. 72, nos. 1–2, pp. 185–195, Apr. 2013.

[7] C. Gohrle, A. Schindler, A. Wagner, and O. Sawodny, "Design and vehicle implementation of preview active suspension controllers," *IEEE Trans. Control Syst. Technol.*, vol. 22, no. 3, pp. 1135–1142, May 2014.

[8] Y. Wu, B. Jiang, and N. Lu, "A descriptor system approach for estimation of incipient faults with application to high-speed railway traction devices," *IEEE Trans. Syst., Man, Cybern., Syst.*, vol. 49, no. 10, pp. 2108–2118, Oct. 2019.

[9] H. Li, X. Jing, H. K. Lam, and P. Shi, "Fuzzy sampled-data control for uncertain vehicle suspension systems," *IEEE Trans. Syst., Man, Cybern., Syst.*, vol. 44, no. 7, pp. 1111–1126, Jul. 2017.

[10] S.-Y. Han, X.-F. Zhong, Y.-H. Chen, and G.-Y. Tang, "Fuzzy guaranteed cost H_∞ control of uncertain nonlinear fuzzy vehicle active suspension with random actuator delay," *Int. J. Fuzzy Syst.*, vol. 21, no. 7, pp. 2021–2031, Oct. 2019.

[11] Z. Fei, X. Wang, M. Liu, and J. Yu, "Reliable control for vehicle active suspension systems under event-triggered scheme with frequency range limitation," *IEEE Trans. Syst.*, to be published, doi: 10.1109/TSMC.2019.2899942.

[12] M. Moradi and A. Fekih, "Adaptive PID-sliding-mode fault-tolerant control approach for vehicle suspension systems subject to actuator faults," *IEEE Trans. Veh. Technol.*, vol. 63, no. 3, pp. 1041–1054, Mar. 2014.

[13] K. Zhang, B. Jiang, X.-G. Yan, and Z. Mao, "Incipient voltage sensor fault isolation for rectifier in railway electrical traction systems," *IEEE Trans. Ind. Electron.*, vol. 64, no. 8, pp. 6763–6774, Aug. 2017.

[14] J. Zhang, A. Amodio, T. Li, B. Aksun-Güvenç, and G. Rizzoni, "Fault diagnosis and fault mitigation for torque safety of drive-by-wire systems," *IEEE Trans. Veh. Technol.*, vol. 67, no. 9, pp. 8041–8054, Sep. 2018.

[15] R. Wang and J. Wang, "Fault-tolerant control with active fault diagnosis for four-wheel independently driven electric ground vehicles," *IEEE Trans. Veh. Technol.*, vol. 60, no. 9, pp. 4276–4287, Nov. 2011.

[16] X. Yu and J. Jiang, "A survey of fault-tolerant controllers based on safety-related issues," *Annu. Rev. Control*, vol. 39, pp. 46–57, Apr. 2015.

[17] Z. Gao, C. Cecati, and S. X. Ding, "A survey of fault diagnosis and fault-tolerant techniques—Part I: Fault diagnosis with model-based and signal-based approaches," *IEEE Trans. Ind. Electron.*, vol. 62, no. 6, pp. 3757–3767, Jun. 2015.

[18] Y. Wu, B. Jiang, and Y. Wang, "Incipient winding fault detection and diagnosis for squirrel-cage induction motors equipped on CRH trains," *ISA Trans.*, to be published, doi: 10.1016/j.isatra.2019.09.020.

[19] Y.-X. Li and G.-H. Yang, "Fuzzy adaptive output feedback fault-tolerant tracking control of a class of uncertain nonlinear systems with nonaffine nonlinear faults," *IEEE Trans. Fuzzy Syst.*, vol. 24, no. 1, pp. 223–234, Feb. 2016.

[20] H. Wang, B. Zhou, and C.-C. Lim, "H_∞ fault-tolerant control of networked control systems with actuator failures," *IET Control Theory Appl.*, vol. 8, no. 12, pp. 1127–1136, Aug. 2014.

[21] S.-Y. Han, Y.-H. Chen, and G.-Y. Tang, "Fault diagnosis and fault-tolerant tracking control for discrete-time systems with faults and delays in actuator and measurement," *J. Frankl. Inst. Eng. Appl. Math.*, vol. 354, no. 12, pp. 4719–4738, Aug. 2017.

[22] Y. Wu, B. Jiang, and N. Lu, "A descriptor system approach for estimation of incipient faults with application to high-speed railway traction devices," *IEEE Trans. Syst., Man, Cybern., Syst*, vol. 49, no. 10, pp. 2108–2118, Oct. 2019.

[23] X. Yu, P. Li, and Y. Zhang, "The design of fixed-time observer and finite-time fault-tolerant control for hypersonic gliding vehicles," *IEEE Trans. Ind. Electron.*, vol. 65, no. 5, pp. 4135–4144, May 2018.

[24] X. Yu, Y. Fu, P. Li, and Y. Zhang, "Fault-tolerant aircraft control based on self-constructing fuzzy neural networks and multivariable SMC under actuator faults," *IEEE Trans. Fuzzy Syst.*, vol. 26, no. 4, pp. 2324–2335, Aug. 2018.

[25] J. Zhang, T. Li, A. Amodio, B. Aksun-Guvenc, and G. Rizzoni, "Fault diagnosis and fault tolerant control for electrified vehicle torque security," in *Proc. IEEE Transp. Electrification Conf. Expo*, Jul. 2016, pp. 27–29.

[26] J. Y. Su and W.-H. Chen, "Model-based fault diagnosis system verification using reachability analysis," *IEEE Trans. Syst., Man, Cybern., Syst*, vol. 49, no. 4, pp. 742–751, Apr. 2019.
[27] Y. Liu, Y. Niu, and J. Lam, "Sliding mode control for uncertain switched systems with partial actuator faults," *Asian J. Control*, vol. 16, no. 6, pp. 1779–1788, Nov. 2014.
[28] Y. Y. Li, H. R. Karimi, Q. Zhang, D. Zhao, and Y. B. Li, "Fault detection for linear discrete time-varying systems subject to random sensor delay: A Riccati equation approach," *IEEE Trans. Circuits Syst. I, Reg. Papers*, vol. 65, no. 5, pp. 1707–1716, May 2018.
[29] Q. K. Shen, B. Jiang, and V. Cocquempot, "Fault-tolerant control for T–S fuzzy systems with application to near-space hypersonic vehicle with actuator faults," *IEEE Trans. Fuzzy Syst.*, vol. 20, no. 4, pp. 652–665, Aug. 2012.
[30] H. Zhang, X. Zheng, H. Yan, Z. Wang, and Q. Chen, "Codesign of event-triggered and distributed H_∞ filtering for active semi-vehicle suspension systems," *IEEE/ASME Trans. Mechatronics*, vol. 22, no. 2, pp. 1047–1058, Apr. 2017.
[31] S. Wen, M. Z. Q. Chen, Z. Zeng, X. Yu, and T. Huan, "Fuzzy control for uncertain vehicle active suspension systems via dynamic sliding-mode approach," *IEEE Trans. Syst., Man, Cybern., Syst.*, vol. 47, no. 1, pp. 24–32, Jan. 2017.
[32] S. Liu, H. Zhou, X. Luo, and J. Xiao, "Adaptive sliding fault tolerant control for nonlinear uncertain active suspension systems," *J. Frankl. Inst. Eng. Appl. Math.*, vol. 353, no. 1, pp. 180–199, Jan. 2016.
[33] H. Li, H. Liu, H. Gao, and P. Shi, "Reliable fuzzy control for active suspension systems with actuator delay and fault," *IEEE Trans. Fuzzy Syst.*, vol. 20, no. 2, pp. 342–357, Apr. 2012.
[34] J. Qiu, M. Ren, Y. Zhao, and Y. Guo, "Active fault-tolerant control for vehicle active suspension systems in finite-frequency domain," *IET Control Theory Appl.*, vol. 5, no. 13, pp. 1544–1550, Sep. 2011.
[35] H. Du and N. Zhang, "H_∞ control of active vehicle suspensions with actuator time delay," *J. Sound Vib.*, vol. 301, nos. 1–2, pp. 236–252, 2006.
[36] R. Isermann, "Model-based fault detection and diagnosis—Status and applications," *Annu. Rev. Control*, vol. 29, no. 1, pp. 71–85, 2005.
[37] P. M. Frank, "Analytical and qualitative model-based fault diagnosis—A survey and some new results," *Eur. J. Control*, vol. 2, no. 1, pp. 6–28, 1996.

Shi-Yuan Han received the M.S. and Ph.D. degrees in computer science and technology from the Ocean University of China, Qingdao, China, in 2009 and 2012, respectively.

From 2011 to 2012, he had been a Visiting Scholar with the School of EECS, Queensland University of Technology, Brisbane, QLD, Australia. In 2012, he joined the University of Jinan, Jinan, China, where he is currently an Associate Professor with the Shandong Provincial Key Laboratory of Network Based Intelligent Computing. His current research interests include the areas of fault tolerant control, vibration control, intelligent transportation systems, time-delay systems, evolutionary computation, networked control systems, and their applications in suspension systems.

Jin Zhou (Member, IEEE) received the B.S. and M.S. degrees in software engineering from Shandong University, Jinan, China, in 1998 and 2001, respectively, and the Ph.D. degree in software engineering from the University of Macau, Macau, China, in 2014.

He is currently a Professor with the Shandong Provincial Key Laboratory of Network Based Intelligent Computing, University of Jinan, Jinan. His current research interests include intelligent transportation systems, evolutionary computation, and other machine learning techniques and their applications in suspension systems.

Yue-Hui Chen received the B.S. degree in control theory from the Department of Mathematics, Shandong University, Jinan, China, in 1985, and the M.S. and Ph.D. degrees in system information science from the Kumamoto University of Japan, Kumamoto, Japan, in 1999 and 2001, respectively.

From 2001 to 2003, he had worked as a Senior Researcher with the Memory-Tech Corporation, Tokyo, Japan. Since 2003, he has been a Member with the Faculty of School of Information Science and Engineering, University of Jinan, Jinan, where he currently the Head of the Computational Intelligence Laboratory. His research interests include optimal control, evolutionary computation, neural networks, fuzzy logic systems, hybrid computational intelligence, computational intelligence grid and their applications in time-series prediction, system identification, intelligent control, intrusion detection systems, Web intelligence, networked control systems, bioinformatics, and systems biology.

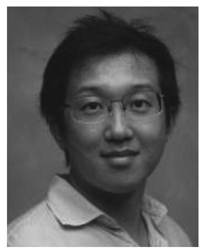

Yi-Fan Zhang (Member, IEEE) received the B.Eng. and M.Eng. degrees in reliability and systems engineering from the Beijing University of Aeronautics and Astronautics, Beijing, China, in 2008 and 2011, respectively, and the Ph.D. degree in data science from the Queensland University of Technology, Brisbane, QLD, Australia, in 2016.

He is currently a Postdoctoral Fellow with CSIRO Agriculture and Food, Queensland Bioscience Precinct, St. Lucia, QLD, Australia. His research interests include artificial intelligence, time series modeling, cloud computing, and the Internet of Things.

Gong-You Tang received the Ph.D. degree in control theory and applications from the South China University of Technology, Guangzhou, China, in 1991.

He is currently a Professor with the College of Information Science and Engineering, Ocean University of China, Qingdao, China. His research interests are in the areas of nonlinear systems, delay systems, large-scale systems, and networked control systems, with emphasis on optimal control, robust control, and fault diagnosis and stability analysis.

Prof. Tang is an Editor of the *Journal of the Ocean University of China* and *Control and the Instruments in Chemical Industry*.

Lin Wang (Member, IEEE) was born in Shandong, China, in 1983. He received the B.Sc. and master's degrees in computer science and technology from the University of Jinan, Jinan, China, in 2005 and 2008, respectively, and the Ph.D. degree in computer science and technology from the School of Computer Science and Technology, Shandong University, Jinan, in 2011.

He is currently an Associate Professor with the Shandong Provincial Key Laboratory of Network-Based Intelligent Computing, University of Jinan. His research interests include classification, hybrid computational intelligence, and mathematical modeling.